



# Coupling creep and damage in concrete through a constant parameter

Marina Bottoni, Frédéric Dufour, Gilles Pijaudier-Cabot

## ► To cite this version:

Marina Bottoni, Frédéric Dufour, Gilles Pijaudier-Cabot. Coupling creep and damage in concrete through a constant parameter. Fracture Mechanics of Concrete and Concrete Structures (FRAMCOS 6), Jun 2007, Catania, Italy. hal-01532829

**HAL Id: hal-01532829**

**<https://hal.science/hal-01532829>**

Submitted on 3 Jun 2017

**HAL** is a multi-disciplinary open access archive for the deposit and dissemination of scientific research documents, whether they are published or not. The documents may come from teaching and research institutions in France or abroad, or from public or private research centers.

L'archive ouverte pluridisciplinaire **HAL**, est destinée au dépôt et à la diffusion de documents scientifiques de niveau recherche, publiés ou non, émanant des établissements d'enseignement et de recherche français ou étrangers, des laboratoires publics ou privés.

Public Domain

# Coupling creep and damage in concrete through a constant parameter

M. Bottoni

*DISTART - Structural Engineering, University of Bologna, Bologna, Italy*

F. Dufour, G. Pijaudier-Cabot

*R&DO, GeM, CNRS, École centrale de Nantes, Nantes, France*

**ABSTRACT:** Coupling between creep and damage is studied in order to properly describe tertiary creep of concrete. Evolution of damage is governed by a strain tensor through an energy norm, obtained by weighting total and elastic strain tensor by means of a constant parameter. In fact, previous analyses show that, if coupling between creep and damage rely upon total strains, tertiary creep occurs too early. In this study, damage model with bilinear constitutive law and Benboudjema's creep model are employed. Numerical simulations provide the structural response after the introduction of the coefficient.

## 1 INTRODUCTION

The failure of quasi-brittle materials under mechanical loading can be divided into two different parts. Initially, diffuse microcracking (damage) occurs in the Fracture Process Zone (FPZ) due to heterogeneities at the micro-scale. Further on micro-cracks coalesce into a macro one yielding strain localization. As the size of the FPZ is related to the microstructure, this type of fracture yields a size effect extensively studied by Bažant since the 70s (Bažant 1976). For prestressed concrete structures for which permanent load level is large, such as in walls of nuclear power plants, the influence of creep on the fracture process should be taken into account. We tackled coupling between creep and failure properties from experimental and numerical point of view keeping in mind the perspective of size effect. Therefore, several analyses have been performed on three point bending tests on a notched beam of three homothetic sizes.

Coupling between creep and damage is well recognized (Mazzotti and Savoia 2003, Proust and Pons 2001, Bažant 1993) in literature. Experimental evidences of interaction between basic creep and damage has been observed on three-point bending tests with several levels of sustained load (Loukili et al. 2001, Omar 2004). Tertiary creep yielding failure has eventually been reached for some of the largest beams and loaded at the highest level. For surviving beams a residual capacity test has been performed to evaluate peak load and fracture energy after three months of creep at different load levels. The conclusion (Omar et al. 2004) of this study is that the bearing capacity is slightly influenced by creep whereas the fracture en-

ergy decrease is not negligible (up to 30%). Therefore we observe a shift towards the LEFM response in the size effect analysis.

Some authors proposed coupled models where concrete damage, humidity variation, and creep strain are considered (see for example Hubert et al. 2001, Ozbolt and Reinhardt 2001). In the present paper, we develop a model to couple creep and damage, whose parameters will be calibrated in the immediate future by interpreting the experimental results in terms of failure due to tertiary creep and fracture energy reduction.

For concrete damage, a strain-based formulation is adopted (Badel 2001), where damage is written in terms of a positive expression of strains, as often assumed in damage models for concrete (Mazars and Pijaudier-Cabot 1989, Di Prisco and Mazars 1996). Creep is described through Benboudjema's model for basic creep (Benboudjema et al. 2005).

In the coupling model, evolution of damage is governed by a strain tensor through an energy norm, obtained by weighting total and creep strain tensors by means of a constant parameter (Mazzotti and Savoia 2002). In fact, previous analyses (Dufour et al. 2006) show that, if coupling between creep and damage is related to total strains, tertiary creep occurs too early and for smaller load levels.

Numerical simulations on a simple structure, obtained after having implemented the model in the finite element *Code-Aster*, are then reported, providing the influence of the coupling parameter on the structural response.

## 2 DAMAGE MODEL

In this work, a simple isotropic damage model with secant unloading is adopted (Badel 2001, Badel 2005). For the state of pure tension, a bilinear stress-strain law is derived; for pure compression the law is linear elastic. Such simplified assumption for material behavior in compression is acceptable, because for beams of our experimental tests collapse is caused essentially by tension stresses, with compressed zones of beam cross-section remaining in the linear range. Material constants are initial elastic Young modulus  $E_0$ , peak strengths in tension  $\sigma_t$  and compression  $\sigma_c$  and softening modulus  $E_1$  (slope of the softening branch).

Damage criterion  $f$  is defined in the following way:

$$f(F^d) = F^d - \kappa \quad (1)$$

where  $F^d$  is the thermodynamic force and threshold  $\kappa$  is defined as:

$$\kappa = \kappa_0 + \kappa_1 \cdot tr(\epsilon) \cdot H(-tr(\epsilon)) \quad (2)$$

being  $H$  the Heaviside function,  $\kappa_0$  and  $\kappa_1$  parameters depending on material strengths and elasticity moduli and  $\gamma$  a dimensionless positive constant:

$$\gamma = -\frac{E_0}{E_1} \quad (3)$$

$$\kappa_0 = \sigma_t^2 \left( \frac{1+\gamma}{2E_0} \right) \left( \frac{1+\nu-\nu^2}{1+\nu} \right) \quad (4)$$

$$\kappa_1 = \sigma_c^2 \frac{(1+\gamma)\nu^2}{(1+\nu)(1-2\nu)} - \kappa_0 \frac{E_0}{(1-2\nu)(\sigma_c)} \quad (5)$$

Through  $\kappa_1$ , concrete confinement is taken into account and contributes to  $\kappa$  only with negative bulk strains (through Heaviside function). In case tension strains prevail, term  $tr(\epsilon)$  is positive and  $\kappa = \kappa_0$ .

In Equation 1, thermodynamic force  $F^d$  is defined as:

$$F^d = \frac{\partial \Phi}{\partial d} \quad (6)$$

where free energy is easily written in the reference system of principal strains:

$$\begin{aligned} \Phi(\epsilon, d) = & \frac{\lambda}{2} tr^2(\epsilon) \left[ H(-tr(\epsilon)) + \frac{1-d}{1+\gamma d} H(tr(\epsilon)) \right] \\ & + \mu \sum_j \hat{\epsilon}_j^2 \left[ H(-\hat{\epsilon}_j) + \frac{1-d}{1+\gamma d} H(\hat{\epsilon}_j) \right] \end{aligned} \quad (7)$$

where  $d$  is damage,  $\lambda$ ,  $\mu$  are Lamé coefficients and  $\hat{\epsilon}_j$  is the  $j$ -th strain component in the principal reference system.

Stresses in the principal reference system are easily derived, since principal directions for strains and

stresses coincide (for demonstration see Badel 2005):

$$\begin{aligned} \hat{\sigma}_j = & \lambda tr(\epsilon) \left[ H(-tr(\epsilon)) + \frac{1-d}{1+\gamma d} H(tr(\epsilon)) \right] \\ & + 2\mu \hat{\epsilon}_j \left[ H(-\hat{\epsilon}_j) + \frac{1-d}{1+\gamma d} H(\hat{\epsilon}_j) \right] \end{aligned} \quad (8)$$

Satisfaction of the criterion states  $f \leq 0$ , and evolution of damage state variable  $d$  is determined by Kuhn-Tucker conditions:

$$\begin{cases} \dot{d} = 0 & \text{if } f < 0 \\ \dot{d} > 0 & \text{if } f = 0 \end{cases} \quad (9)$$

It is found that, to have  $f = 0$ , i.e. the condition for evolution of damage, damage  $d$  is given by:

$$d = \frac{1}{\gamma} \left( \sqrt{\frac{1+\gamma}{\kappa} W(\epsilon)} - 1 \right) \quad (10)$$

with positive energy  $W(\epsilon)$ :

$$W(\epsilon) = \frac{\lambda}{2} tr^2(\epsilon) H(tr(\epsilon)) + \mu \sum_j \hat{\epsilon}_j^2 H(\hat{\epsilon}_j) \quad (11)$$

Reference is done to Badel 2005 for the computation of the material tangent matrix, required by the Newton-Raphson solution method. It can be shown, tangent matrix can be expressed in a close form.

Crack closure is also taken into account by the model through the terms  $H(-\hat{\epsilon}_j) + \frac{1-d}{1+\gamma d} H(\hat{\epsilon}_j)$  and  $H(-tr(\epsilon)) + \frac{1-d}{1+\gamma d} H(tr(\epsilon))$ . A tensile loading, for instance, causes the material to damage i.e. coefficient  $\frac{1-d}{1+\gamma d} \neq 1$ ; if later on the sign of the load is inverted and the material becomes compressed, initial stiffness is restored through the Heaviside function.

## 3 CREEP MODEL

In the present paper, Bemboudjema's model for basic creep is adopted.

The model (Benboudjema et al. 2005, Benboudjema 2002) attributes the phenomenon of creep to water movement in the cement paste and is described through the combination of hydrates elastic behavior and water viscous behavior.

First, total strains are split into an elasto-damaged part  $\epsilon_e$  and a (basic) creep part  $\epsilon_{cr}$ :

$$\epsilon = \epsilon_e + \epsilon_{cr} \quad (12)$$

Creep strains are then decomposed in reversible and irreversible and then in their spherical and deviatoric part, so obtaining:

$$\epsilon_{cr} = \epsilon_{cr}^{sr} + \epsilon_{cr}^{si} + \epsilon_{cr}^{dr} + \epsilon_{cr}^{di} \quad (13)$$

where strain tensors  $\epsilon_{cr}^{sr}$ ,  $\epsilon_{cr}^{si}$ ,  $\epsilon_{cr}^{dr}$ ,  $\epsilon_{cr}^{di}$  are spherical reversible, spherical irreversible, deviatoric reversible and deviatoric irreversible, respectively. Components of these four tensors are the state variables of the creep model.

For stresses an analogous splitting is operated, with indexes  $s$  and  $d$  indicating spherical and deviatoric part of stresses:

$$\boldsymbol{\sigma} = \boldsymbol{\sigma}^s + \boldsymbol{\sigma}^d \quad (14)$$

Parameters of the model are:

- $k_{is} \rightarrow$  Spherical irreversible stiffness
- $\eta_{rs} \rightarrow$  Spherical reversible viscosity
- $\eta_{is} \rightarrow$  Spherical irreversible viscosity
- $k_{rd} \rightarrow$  Deviatoric reversible stiffness
- $\eta_{rd} \rightarrow$  Deviatoric reversible viscosity
- $\eta_{id} \rightarrow$  Deviatoric irreversible viscosity

Assumption of the model is that, deviatoric strains depend only on deviatoric stresses and spherical strains depend only on spherical stresses. Four differential equations (not reported here) describe the physical problem.

The set of differential equation of the model can be numerically solved by assuming a linear approximation in the time interval for stresses and relative humidity. For each component of the creep strain tensor (in the sense of the split given by Equation 13), an equation of the following kind is then obtained (and written here for  $\varepsilon_{cr,n}^{dr}$ ):

$$\varepsilon_{cr,n}^{dr} = \varepsilon_{cr,n-1}^{dr} + \mathbf{a}_n^{dr} + \mathbf{b}_n^{dr} \boldsymbol{\sigma}_{n-1}^d + \mathbf{c}_n^{dr} \boldsymbol{\sigma}_n^d \quad (15)$$

where index  $n$  stands for  $n$ -th timestep. By summing Equation (15) with the analogous ones for  $\varepsilon_{cr}^{di}$ ,  $\varepsilon_{cr}^{sr}$ ,  $\varepsilon_{cr}^{si}$ , general equation for updating total creep strain tensor is obtained:

$$\varepsilon_{cr,n} = \varepsilon_{cr,n-1} + \mathbf{A}_n + \mathbf{B}_n \boldsymbol{\sigma}_{n-1} + \mathbf{C}_n \boldsymbol{\sigma}_n \quad (16)$$

Matrices  $\mathbf{B}_n$ ,  $\mathbf{C}_n$ ,  $\mathbf{b}_n^{dr}$ ,  $\mathbf{c}_n^{dr}$  and vectors  $\mathbf{A}_n^{dr}$ ,  $\mathbf{a}_n$  depend on timestep  $\Delta t_n = t_n - t_{n-1}$ , relative humidity  $h$  and creep strains. For their computation reference is made to Le Pape 2004 or Benboudjema 2002.

## 4 COUPLING CREEP AND DAMAGE

### 4.1 General idea

Coupling between creep and damage is operated by modifying strains causing damage evolution. In case no coupling is assumed, creep strains must have no role in structure damaging; under constant load and even for high load levels, structure deformation would grow with decreasing speed, eventually up to an asymptotically finite value. Nonetheless, we know the phenomenon of tertiary creep can take place when load level is elevated, with deformation growing with increasing speed and so leading structure to collapse. It is then necessary to connect creep with material degradation, described by damage. A possibility is to let damage be governed by total strains; in this

case coupling would be total, and the worst case for the structure. Previous works show, in fact, total coupling tends to underestimate structure ultimate capacity, (Dufour et al. 2006, Mazzotti and Savoia 2003). However, a partial coupling could happen, if only a portion of creep strains contributes to damage. In this work we suppose damage evolving to be controlled by following strain tensor  $\check{\varepsilon}$ , obtained by weighting total and elasto-damaged strain tensors (see also Mazzotti and Savoia 2002):

$$\check{\varepsilon} = (1 - \beta)\varepsilon + \beta\varepsilon_e \quad (17)$$

which can also be written as:

$$\check{\varepsilon} = \varepsilon - \beta\varepsilon_{cr} \quad (18)$$

where  $\varepsilon$ ,  $\varepsilon_{cr}$  and  $\varepsilon_e$  have the same meaning as in Equation 12 and parameter  $\beta$  is constant.

Total coupling or absence of coupling are obtained as special cases with coefficient  $\beta$  assuming values of 0 and 1, respectively.

### 4.2 Numerical procedure

A Newton-Raphson or modified Newton-Raphson solution method is adopted, providing the typical incremental-iterative numerical frame of non-linear problems. The complete description of the numerical procedure is graphically exemplified in Figure 1. Indexes  $n$  and  $i$  indicate timestep (increment) and general Newton-Raphson iteration, respectively. Usually, index  $n$  of present timestep is not reported for sake of simplicity and  $q_i$  indicates a certain variable at iteration  $i$  of the current timestep  $n$ . Tolerance  $\omega_{NR}$  is the accepted relative error on residual forces.

Update of state variables as well as computation of stresses is done for each iteration in the single Gauss point, where total strains  $\varepsilon_i$  (and displacements  $U_i$ ) are supposed to be known from linearized Newton-Raphson problem. State variables of the coupled model are damage  $d$  and components of each creep strain tensors  $\varepsilon_{cr}^{sr}$ ,  $\varepsilon_{cr}^{si}$ ,  $\varepsilon_{cr}^{dr}$ ,  $\varepsilon_{cr}^{di}$  (see Equation 13).

The numerical procedure is composed by following steps:

- 1 Computation of weighted strains  $\check{\varepsilon}_i$  controlling damage, according to Equation 17.
- 2 Update of damage, which is operated by first writing damage criterion  $f$  as a function of weighted strains and then the Kuhn-Tucker condition  $f = 0$ :

$$\frac{1 + \gamma}{(1 + \gamma d)^2} W(\check{\varepsilon}) = \kappa \quad (19)$$

The new level of damage is then found:

$$d_{test} = \frac{1}{\gamma} \left( \sqrt{\frac{1 + \gamma}{\kappa} W(\check{\varepsilon})} - 1 \right) \quad (20)$$

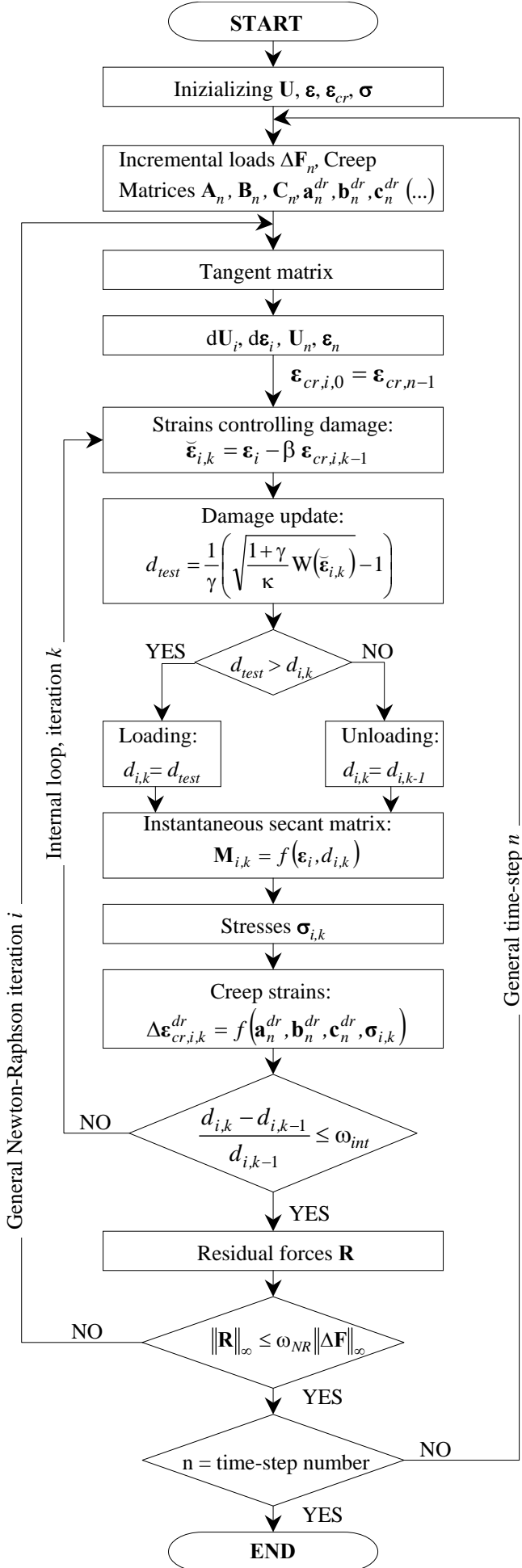


Figure 1. Scheme of the algorithm in the frame of the incremental-iterative procedure.

where positive energy  $W(\tilde{\epsilon})$  is written as:

$$W(\tilde{\epsilon}) = \frac{\lambda}{2} tr^2(\tilde{\epsilon}) H(tr(\tilde{\epsilon})) + \mu \sum_j \hat{\epsilon}_j^2 H(\hat{\epsilon}_j) \quad (21)$$

Crack closure in Equation 21 is still controlled by total strains by arguments of Heaviside function.

Computation of  $\tilde{\epsilon}_i$  is not exact at this point. In fact, tensor  $\tilde{\epsilon}_i$  depends on stresses, which are still unknown. Consequently, an internal loop (with tolerance  $\omega_{int}$ ) is required as shown in Figure 1; creep strains are initialized with their value at previous time step  $\tilde{\epsilon}_{n-1}$ . In the particular case of total coupling no loop is necessary, since  $\tilde{\epsilon}_i$  are known and equal to total strains  $\epsilon_i$ .

3 Computation of stresses at  $t_n$  is operated by first writing relationship between stresses and instantaneous strains:

$$\sigma_n = \mathbf{M}(\epsilon_n - \epsilon_{cr,n}) \quad (22)$$

where  $\mathbf{M}$  at present iteration  $i$  is the instantaneous secant matrix, defined as:

$$\mathbf{M} = \left\{ \frac{\partial \sigma}{\partial \epsilon_e} \right\}_{d=cst} \quad (23)$$

After substitution of Equation 16 into Equation 22, increment of creep strains in  $\Delta t_n = t_n - t_{n-1}$  is found as:

$$\Delta \epsilon_{cr,n} = (\mathbf{1} + \mathbf{C}_n \mathbf{M})^{-1} \cdot \quad (24)$$

$$[\mathbf{A}_n + \mathbf{B}_n \sigma_{n-1} + \mathbf{C}_n \mathbf{M}(\epsilon_n - \epsilon_{cr,n-1})]$$

Stresses  $\sigma_n$  at time  $t_n$  are then known through Equation 22.

4 Update of creep strains through Equation 15.

Values assumed from creep strains at this point is not definitive, since they depend on damage through instantaneous secant matrix  $\mathbf{M}$ . Therefore, computational steps have to be repeated from point 1, up to convergence in the value of damage and creep strains. Exception is given by cases of total or absence of coupling, for which no iteration is needed.

Convergence is evaluated for two successive values of damage and then reached when:

$$\frac{d_k - d_{k-1}}{d_{k-1}} \leq \omega_{int} \quad (25)$$

where index  $k$  indicates iteration in the internal loop.

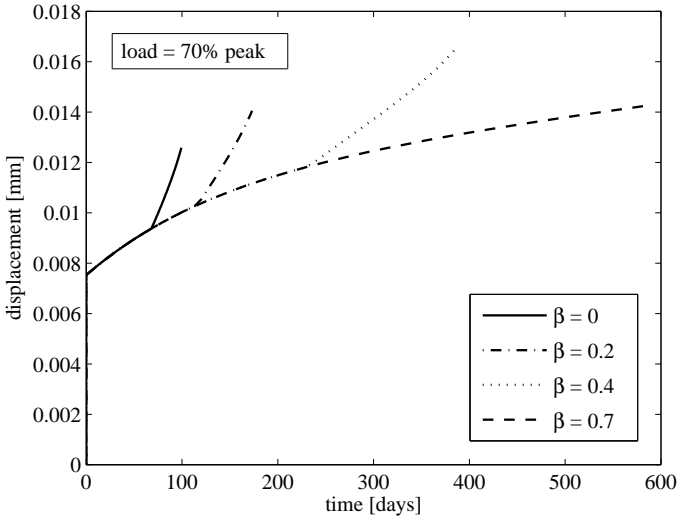


Figure 2. Variation of coefficient  $\beta$  for a load level fixed to 70% of instantaneous peak.

## 5 RESULTS

### 5.1 Tension test on a single finite element

First tests of the model were lead on a single bi-linear four-noded plane stress finite element. The element was subject to a pure tension loading constant in time. Load is quantified as a percentage of peak-load. Results are given in term of displacements versus time in a linear scale. When possible (no collapse occurs), finite element is tested up to 600 days (about 20 months). Temperature has been taken constant and equal to its reference value. Computation parameters are reported in Table 1.

In Figures 2 and 3 effect of variation of new parameter  $\beta$  is observed. All curves coincide, until the process of material damage begins and tertiary creep starts, leading very quickly to collapse. In fact, no structural redistribution is possible in one single element subject to a state of pure tension. Tertiary creep is identifiable in diagrams by the fast increase in slope. Influence of  $\beta$  in the evolution of element de-

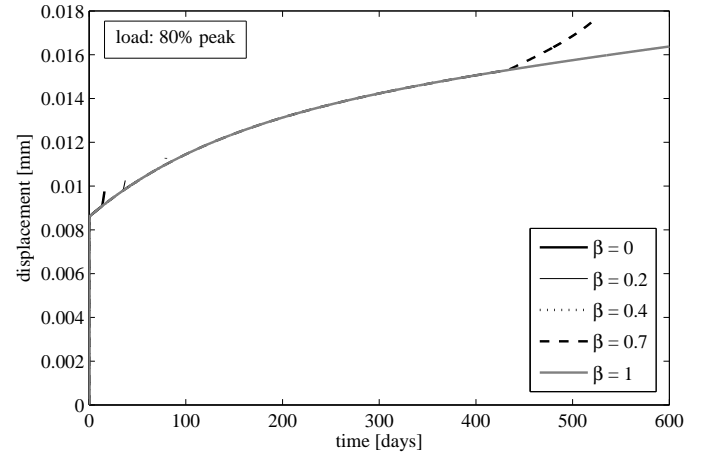


Figure 3. Variation of coefficient  $\beta$  for load level fixed to 80% of instantaneous peak.

formation can be summarized as follows:

- 1 beginning of damaging process and, consequently, of tertiary creep, occurs later;
- 2 when damage process starts later, slope of displacement-time curve is less steep.

Analogous observations can be made from dual diagrams of Figures 4 and 5, showing effect of load variation for a fixed value of  $\beta$ . With lower load levels, slope of displacement-time curve is less steep and begins later because damage increase is slower.

As for the first point, time is the most evident parameter governed by coefficient  $\beta$ . This observation agrees to experimental reality, since as we know, when tertiary creep starts, structures where positive stresses play an important role, such as beams subject to flexural loads, tend to collapse very fast (brittle behavior). Time comes to be an important factor, if a calibration of the coupling parameter is figured out.

Finally, a first test has been performed to see how tolerance  $\omega_{int}$  influences results. Two computations with  $\beta = 0.4$  and load set to 70 % have given the same results in term of displacement-time behavior, when tolerances have been set to  $10^{-5}$  and to  $10^{-1}$ . This is due to the presence of Newton-Raphson iterations

Table 1. Material and environmental constants adopted in numerical tests.

Description	Symbol	Value
Young elasticity modulus [GPa]	$E_0$	31
Poisson ratio	$\nu$	0.2
Tensile strength [MPa]	$\sigma_t$	3
Compressive strength [MPa]	$\sigma_c$	30
Softening modulus [GPa]	$E_1$	-6
Sph. reversible stiffness [MPa]	$k_{rs}$	$6.00 \cdot 10^4$
Sph. irreversible stiffness [MPa]	$k_{is}$	$3.00 \cdot 10^4$
Sph. reversible viscosity [MPa · s]	$\eta_{rs}$	$5.95 \cdot 10^8$
Sph. irreversible viscosity [MPa · s]	$\eta_{is}$	$2.40 \cdot 10^{10}$
Dev. reversible stiffness [MPa]	$k_{rd}$	$3.40 \cdot 10^4$
Dev. reversible viscosity [MPa · s]	$\eta_{rd}$	$4.08 \cdot 10^{11}$
Dev. irreversible viscosity [MPa · s]	$\eta_{id}$	$2.33 \cdot 10^{12}$
Temperature [°C]	$T$	20
Ref. Temperature [°C]	$T_{ref}$	20

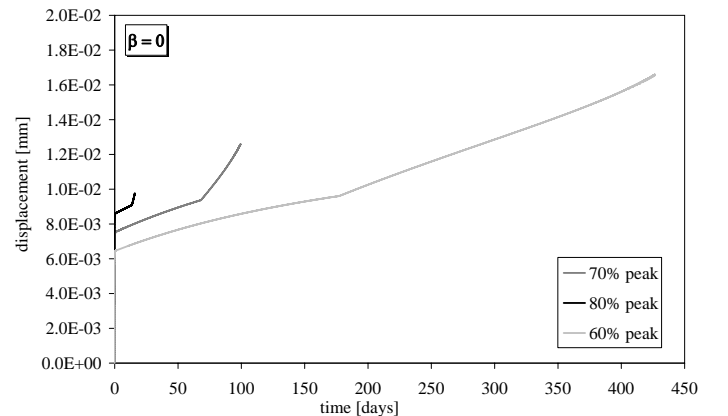


Figure 4. Variation of load level with  $\beta = 0$ .

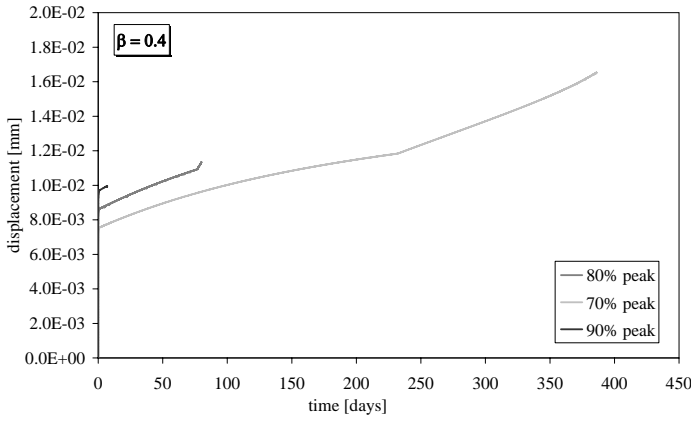


Figure 5. Variation of load level with  $\beta = 0.4$ .

externally to loops in Gauss points; precision for the overall procedure is then governed by the outer loop. This is very true and even trivial but computational time variation would be a good factor to look at. In our case, it was more convenient to take a high precision for the inner loop, since this enhances convergence. With tolerance set to  $10^{-1}$ , convergence is obtained only reducing time step length and computational time was 1310 seconds; with tolerance set to  $10^{-5}$ , computational time resulted in 1230 seconds. The gap could be much wider in case of a more complex structure; it is then significant to determine the more convenient value for  $\omega_{int}$  for our next analyses, which could be quite time-consuming since they will involve non local damage, with a much greater number of dof's. For the moment however, we make use of a modified Newton-Raphson method, adopting the elastic matrix instead of the tangent matrix. Tangent matrix, quite difficult to derive for a three-dimensional law, is implemented only in the total coupling case. Possibly, the convenience in assuming a higher or smaller tolerance will be different, once tangent matrix will be available for partial coupling too.

### 5.2 Structural response on three-point bending test

Two computations have then been performed onto a beam under three-point bending. Loadings have been kept constant in time. As usual to exploit structural symmetry, only half of the beam has been analyzed. Limitedly to this introductory work, a local model has been used in spite of the presence of material softening behavior; for this reason, mesh is very coarse (Figure 6) since damage will localize in a single element band which should be as wide as the FPZ. Beam geometry is the same as the largest beam described in (Loukili et al. 2001), with distance between supports equal to 120 cm, depth 40 cm, width 10 cm, and vertical cut 6 cm. However, our purpose was not to reproduce experimental data, but begin to understand also structural behavior under the influence of coefficient  $\beta$ .

Still with reference to Figure 6, half of the total vertical load is applied at point  $P23$ ; at point  $P18$  vertical displacement is constrained to zero; at points  $P23$ ,  $P20$ ,  $P22$  horizontal displacements are imposed to be

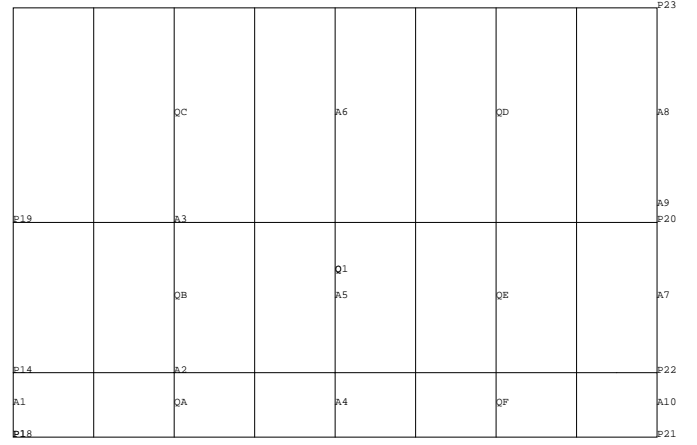


Figure 6. Geometry and meshing of the beam under three point-bending.

zero, too; instead, point  $P21$  is free to move in both horizontal and vertical direction to simulate a vertical cut, which forces collapse crack to take place in the center of the beam. Assumed constants for concrete are the same as in Table 1.

In Figure 7 deflection-time curves are depicted for two values of softening modulus  $E_1$ . Curves arrested due to lack of convergence before a significant increase in slope, which is presumably the reason for which the procedure has not converged and then to be expected after interruption. The two curves differentiate themselves gradually. Structure is expected to be damaged, since parameter  $E_1$  gains a meaning only when damage is different from zero in some region of the spatial domain. Gradual increase of displacement together with non-zero value of damage is probably due to redistribution capabilities of the structure in bending, in opposition to a single element in tension.

## 6 CONCLUSIONS

A partial coupling of Bemboudjema's creep model and damage model has been implemented in Electricité De France's finite element code *Code Aster*. Coupling has been introduced through a constant parameter  $\beta$ ; this intervenes in determining the amount

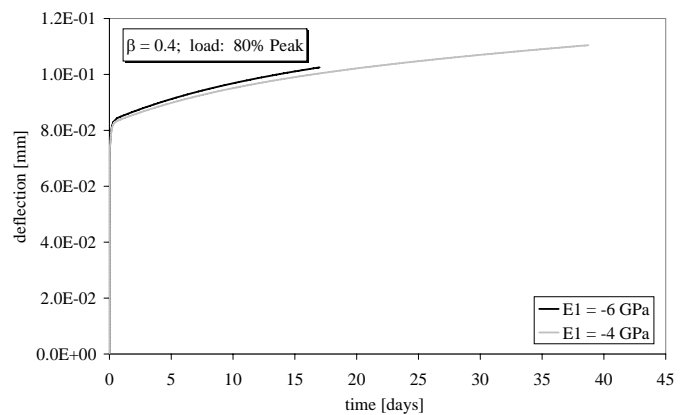


Figure 7. Deflection-time curve for the beam under three point-bending.

of creep strains on which damage evolution depends.

First tests on a single finite element have given positive results. With different values of introduced coefficient  $\beta$ , damaging of the element is delayed. Beginning of damaging coincide with beginning of tertiary creep. A few results have been also obtained from numerical simulations on a simple structure. There, a structural effect is observed and presence of damage does not provoke the immediate beginning of tertiary creep, as happens in the single element.

The coupling of creep and damage in the non local damage frame is under development in order to simulate quantitatively the tertiary creep observed during creep tests and the size effect analyzed afterwards on surviving structures.

## 7 ACKNOWLEDGEMENTS

This work was partially supported from the EU project "Degradation and Instabilities in Geomaterials with Application to Hazard Mitigation" (DIGA-HPRN-CT-2002-00220) in the framework of the Human Potential Program, Research Training Networks.

## REFERENCES

- Badel, P. (2001). *Contributions à la simulation numérique de structures en béton armé*. Ph. D. thesis, Université Pierre et Marie Curie. (in French).
- Badel, P. (2005). *Loi de comportement ENDO ISO BETON*. EDF-R&D/MMC. Manuel de Référence du Code Aster, Document R7.01.14 (in French).
- Bazant, Z. P. (1976). Instability, ductility and size effect in strain-softening concrete. *J. Eng. Mech.* 103, 331–344.
- Bazant, Z. P. (1993). Current status and advances in the theory of creep and interaction with fracture. In Z. P. Bazant and I. Carol (Eds.), *Proc., 5th Int. RILEM Symp. on Creep and Shrinkage of Concrete*, pp. 291–307. Barcelona, E&FN Spon, London.
- Benboudjema, F. (2002). *Modelisation des deformations differées du beton sous sollicitations biaxiales. Application aux enceintes de confinement de bâtiments reacteurs de centrales nucleaires*. Ph. D. thesis, Université de Marne la Vallée, U.F.R. de Sciences et Technologies. (in French).
- Benboudjema, F., F. Meftah, and J. Torrenti (2005). Interaction between drying, shrinkage, creep and cracking phenomena in concrete. *Eng. Struc.* 27, 239–250.
- Di Prisco, M. and J. Mazars (1996). Crush-crack: A non-local damage model for concrete. *Mech. Cohesive-Frict. Mater* 1, 321–347.
- Dufour, F., G. Pijaudier-Cabot, T. Baxevanis, R. Desiassyfayanty, and M. Omar (2006). Creep-damage coupling. In *Proceedings of USNCTAM 2006*.
- Hubert, F. X., N. Burlion, and J. F. Shao (2001). Consequences of dessication on mechanical damage of concrete. In R. de Borst, J. Mazars, J. Pijaudier-Cabot, and J. G. M. van Mier (Eds.), *Proc., FramcosIV*, Volume 1, pp. 223–230. Paris, Elsevier, New York.
- Le Pape, Y. (2004). *Relation de comportement UMLV pour le fluage propre du bétons*. EDF-R&D/MMC. Manuel de Référence du Code Aster, Document R7.01.06 (in French).
- Loukili, A., M. Omar, and G. Pijaudier-Cabot (2001). Basic creep of ultra high strength concrete – experiments and modeling. In Z. P. Bazant, F.-J. Ulm, and F. H. Whitmann (Eds.), *Proc. of Concreep 6*, pp. 545–550. Cambridge, Elsevier, Amsterdam. Paper H3/4.
- Mazars, J. and G. Pijaudier-Cabot (1989). Continuum damage theory – application to concrete. *J. Eng. Mech. Div.* 115(2), 345–365.
- Mazzotti, C. and M. Savoia (2002). Nonlinear Creep, Poisson's Ratio, and Creep-Damage Interaction of Concrete in Compression. *ACI Materials Journal*, 450–457.
- Mazzotti, C. and M. Savoia (2003). Nonlinear creep damage model for concrete under uniaxial compression. *ASCE J. Engineering Mechanics*, 1065–1075.
- Omar, M. (2004). *Deformations différées du béton: Étude expérimentale et modélisation numérique de l'interaction fluage endommagement*. Ph. D. thesis, École centrale de Nantes. (in French).
- Omar, M., K. Haidar, A. Loukili, and G. Pijaudier-Cabot (2004, April). Creep load influence on the residual capacity of concrete structure: Experimental investigation. In *Fracture Mechanics of Concrete Structure (Framcos)*, pp. 605–612.
- Ozbolt, J. and H. W. Reinhardt (2001). Creep-cracking of concrete - three dimensional finite element model. In Z. P. Bazant, F.-J. Ulm, and F. H. Whitmann (Eds.), *Proc. of Concreep 6*, pp. 221–228. Cambridge, Elsevier, Amsterdam.
- Proust, E. and G. Pons (2001). Macroscopic and microscopic behavior of self-compacting concrete creep and shrinkage. In Z. P. Bazant, F.-J. Ulm, and F. H. Whitmann (Eds.), *Proc. of Concreep 6*, pp. 569–574. Cambridge, Elsevier, Amsterdam.